Preprint Volume, 26th Conference on Radar Meteorology, AMS, Norman, OK, May 24-28, 1993.

THREE-DIMENSIONAL KINEMATIC AND MICROPHYSICAL EVOLUTION OF FLORIDA CUMULONIMBUS

Sandra E. Yuter and Robert A. Houze, Jr.

Department of Atmospheric Sciences
University of Washington
Seattle, WA

1. INTRODUCTION

The Convection and Precipitation/Electrification Experiment (CaPE) (Foote, 1991) was held in east central Florida from 8 July to 18 August 1991 to document Florida cumulonimbus. The sensor platforms from CaPE used for this study are the National Center for Atmospheric Research CP2, CP3 and CP4 radars and the South Dakota School of Mines and Technology T-28 research aircraft. The CP3 and CP4 C-band radars were separated by a 23 km baseline and scanned in coordinated dual-Doppler mode. The CP2 radar provided dual-polarization radar data, and the T-28 supplied flight-level data from cloud penetrations.

On 15 August 1991, an eastward moving north-south line of convection formed near Melbourne, Florida. The storm was initiated by the interaction of the sea breeze and an outflow from a thunderstorm further inland. The southern end of the line was in the southern dual-Doppler lobe of the C-band radars, which afforded the opportunity for high time-resolution coverage of the development of the storm from initiation, through mature convection, and into transition toward a stratiform stage. Additionally, CP2 scanned the region for the initial period of storm development.

The goal of this research is to understand how the precipitation mechanisms in Florida cumulonimbus evolve from an early convective stage to the mature stage, in which the storms tend toward a more stratiform structure The storm of 15 August 1991 exhibited such a complex and detailed multi-cellular structure in space and time that it was difficult to characterize using traditional methods such as selected cross-sections and plots of a variable's mean value vs. height. In order to describe the ensemble properties of the storm, a new method of viewing the data was necessary. We introduce a plot called a *three-dimensional histogram* for three variables derived from the radar data analysis: radar reflectivity (Z), vertical velocity (w) and differential reflectivity (ZDR). These plots present a concise statistical summary of the salient features of the precipitation structure and air motions in a complex multi-cellular cumulonimbus.

2. DATA AND METHODOLOGY

Seven volumes of radar data from the time period of 21:23-22:37 GMT were used to characterize the storm. Five of the radar volumes contain dual-Doppler data from the C-band radars. The two remaining volumes are from CP2 and coincide in time with the first two dual-Doppler volumes. All the volumes required approximately 3 min of scanning time. Dual-Doppler analysis was performed on the C-band radar volumes using conventional methods (following Biggerstaff and Houze, 1991). Radial velocity and radar reflectivity data from each of the C-band radars were interpolated to a Cartesian grid covering 40 km x 39 km with 0.5 km spacing in the horizontal and 0 - 17.2 km (MSL) with 0.4 km spacing in the vertical.

Three dimensional histograms were constructed from the analyzed data to summarize all the information about a variable A in a given radar volume in a single contour plot. To obtain this plot, the data are stratified by height only. The horizontal locations of the data are ignored. Only the frequency of occurrence of A at a given height is considered. The coordinates of the plot are A and height z. The percent frequency of occurence at a given height is contoured (i.e. number of data points at a given level with a given value of A divided by the total number of data points at that level, expressed as a percent). We call this plot a three-dimensional histogram since it shows the topography of the surface created by stacking histograms of A for each height z one above the other.

To illustrate the concept of a three-dimensional histogram we will first consider a simple example of a volume containing a hard-boiled egg. For the variable A we take the color of the constituent material, which is white for the egg white and yellow from the egg yolk. We divide the volume the egg occupies into a regular cartesian grid and then construct a histogram at each level in the grid by counting the number of points that fall into the white and yellow bins. There will also be some grid points outside the egg; these will count as no data points. To produce the plot, we first compute a histogram for each level in the volume and normalize by the number of data points at that level. Each histogram indicates the percent of data points at that level occupied by white or yellow material. Next, we stack the set of histograms in a plot with height as ordinate and color (the two values white and yellow) as the abcissa and contour the resulting field. At the middle height of the egg, the histogram would show some of the data points in the yellow bin and the remainder in the white. Above and below the height of the egg yolk, the plot would have 100% of data in the white bin. Note that the effect of the narrowing of the egg with height is removed by normalizing the histograms by the number of data points at each height. Some information about shape is lost by normalizing at each height but it makes the plot easier to interpret.

Three-dimensional histograms of Z and w were made for each of the five dual-Doppler volumes (Fig. 1). These plots were constructed, as outlined in the egg example above, for the static 40 x 39 x 17.2 km radar volume grid. Since each volume contains many cells at different stages of their lifecycle, the plots show the ensemble properties of the group of cells. The contour interval for the plots is 5% with the 10% contour highlighted. Additionally, the 1% contour is included to show the behavior of the outlyers of the distribution.

3. REFLECTIVITY AND VERTICAL VELOCITY: STORM EVOLUTION

The evolution of the 15 August 1991 cumulonimbus system is indicated by the time series of three-dimensional histograms of Z and w in Fig. 1. Interesting features can be seen

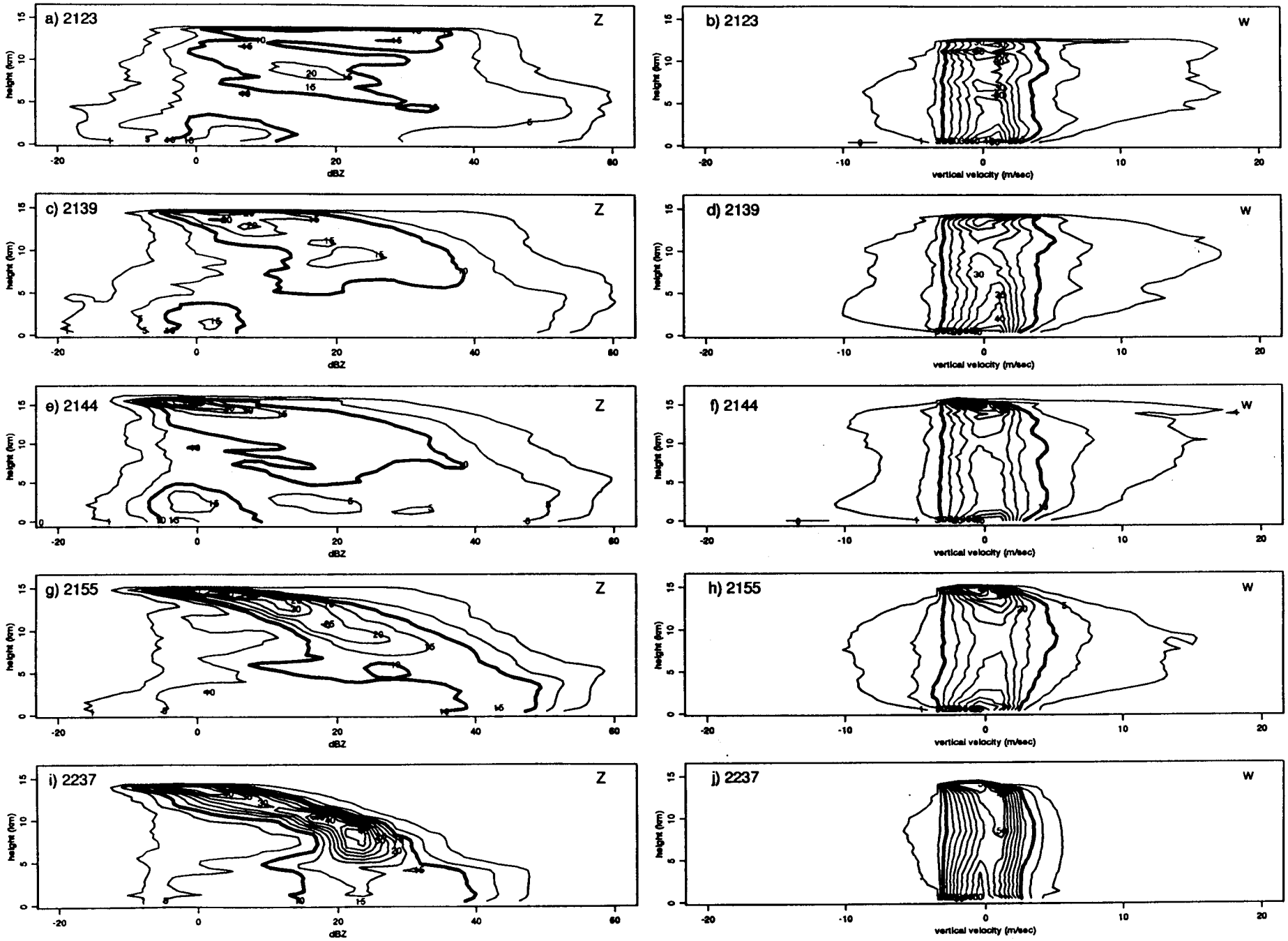

Figure 1. Three-dimensional histograms of radar reflectivity (Z) and vertical velocity (w) from 15 August 1991. Contours are of percentage frequency of occurence of a value at a given height. Data contour interval is 5% starting at 5%. The 10% contour is highlighted and the 1% contour is included to show distribution outlyers.

as the histograms evolve in time and at a given time by comparing radar reflectivity and radial velocity for the same volume.

The left column of Figure 1 is the time series of three-dimensional histograms of radar reflectivity. Overall, the distribution of Z starts out wide and heterogeneous and becomes narrow and unimodal. The 1% contour exhibits a maximum at approximately 5 km in all the radar reflectivity histograms. This consistent enhancement of reflectivity in all time periods is evidently associated with the change of phase of precipitation at the 0 deg C level.

The right column of Figure 1 is the time series of three-dimensional histograms of vertical velocity. The shape of the three dimensional histograms of w indicates that the bulk of the volume of echo is characterized by near zero vertical velocity. This fact has important cloud microphysical implications since it implies that most of the precipitation particles were growing in the presence of weak vertical velocities, even when the storm was in a very active convective stage. Vertical velocities greater than 5 m/s are rare, and values ~ 10 m/s are extremely infrequent. However, although they account for only a small percentage of the volume, the stronger drafts are of great interest since they strongly influence the precipitation processes by generating precipitation particles, and they are the primary agents in the vertical transport of mass, energy and momentum. The remainder of this section is organized around the times represented in the figure.

2123: The convection in the observational domain was in an early stage. Radar echo first appeared behind the eastward moving outflow at 2100 and was augmented by the collision of the outflow and sea breeze convergence lines at 2117. By 2123, some cells had reached heights >10 km, and above the 0 deg C (~ 5 km) level cells were glaciated, as indicated by the ZDR data (not shown). Echoes at low levels (0-5 km) were reaching maxima of 55-60 dBZ (Fig. 1a). However, these echoes accounted only for 1 percent of the data points at a given level. Most of the echo at low levels was quite weak. The most frequently occurring values were in the range of –2 to +16 dBZ. The three-dimensional histogram of vertical velocity (Fig 1b) shows that the most frequently occurring values of vertical velocity were near zero. The mean w was positive throughout the troposphere. However, a wide range of velocities was occurring. The 1% contours show the behavior of the extreme vertical velocities in the strong cells of the echo pattern. Strong updrafts ~15 m/s were found from 5 km altitude upward to echo top. These updrafts were evidently producing a wide range of ice particle types and sizes with a corresponding wide range of reflectivities. At this time, 40 dBZ echoes were reaching the 15 km level, and between 5 and 15 km altitude the 10% contour of the three-dimensional Z histogram covered a wide range of reflectivities (from 0 to nearly 40 dBZ). Downdrafts were also present at all levels. The strongest downdrafts, indicated by the 1% contour in the three-dimensional w histogram, were ~–8 m/s and were at 5-6 km altitude.

2139: Inspection of the horizontal and vertical cross sections of Z and w at this time revealed an ensemble of strong updrafts and downdrafts associated with strong reflectivity cells. Horizontal and vertical cross sections suggest that the drafts had more the appearance of bubbles than jets of convection. The strongest updrafts were at upper levels. Strong, precipitation-loaded downdrafts were present at low levels (Fig. 1d). The strongest updrafts (indicated by the 1% contour) were 17 m/sec at 10 km. The strongest downdrafts were beginning to show a bimodal character, with strong (8 m/s) upper-level downdrafts at 10 km and low-level (10 m/s) precipitation-driven downdrafts at 3 km. These values of vertical velocity are consistent with flight-level data on a south to north penetration along the line of the convection made by the T-28 aircraft starting at 2129 (Detweiler, personal communication). The 10% contour aloft (i.e. above 10 km) in the reflectivity histogram (Fig. 1c) displays the beginning of a trend toward narrowing into a diagonal zone in the three-dimensional histogram, which reaches its extreme at the time of Fig. 1i. Figs. 1a, c, e, g, and i show the progression toward this pattern. The diagonal signature indicates a rather uniform reflectivity at a given height and an increase of reflectivity downward. Evidently, as the overall echo pattern represented by the three-dimensional histogram became less strongly convective, the larger, denser, and more reflective ice particles fell from high levels. Thus the wide spectrum of reflectivities seen at high levels in Fig. 1a narrowed in time as the precipitation evolved from convective, with ice present in a variety of sizes and types with no one category predominating, toward a structure that represented a transitional phase, on the way to becoming stratiform and thus more homogenous in ice types and sizes.

2144: The horizontal cross-section at 10 km revealed that the radar echo had filled in between the cells along the N-S line with most cells 10 km in height. Low levels were characterized by intense updrafts and precipitation loaded downdrafts. At upper levels, intense downdrafts surrounded the upper continuation of intense updrafts from lower levels. The three-dimensional histogram of w (Fig 1f) shows that the peak updrafts were still concentrated aloft, reaching their maxima at 10–15 km. The 1% contour shows a strongly bimodal distribution of downdrafts in height. Upper-level downdrafts ~-10 m/s were most frequent at 12 km and at 2 km height. The upper-level downdrafts appear at the level of strongest updrafts. This behavior, together with the observation (from horizontal and vertical cross-sections) that upper-level downdrafts are typically located immediately adjacent to the updrafts, is consistent with the notion that the upper-level downdrafts were forced when the divergent outflow from the updraft tops converges with the ambient air near the tropopause, and air is forced downward (Hemsfield and Schotz 1985, Smull and Houze 1987). The three-dimensional histogram of reflectivity at this time (Fig. 1e)was not much changed from that at 2139. The sharp peak in concentration centered at 0 dBZ and 15 km was a consequence of the smaller number of data points at that height.

2155: This time could be considered the beginning of the dissipation stage of the system. Updrafts at low levels were less numerous and weaker compared to previous times. The mean surface rain rate over the whole echo region was at a maximum. The three-dimensional histogram of reflectivity (Fig 1g) reflects the onset of heavy rain, as the most frequently occuring low altitude values of dBZ had increased from near 0 dBZ to 35-45 dBZ. The radar echo in the ice (above 5 km) was becoming more stratiform, as evidenced by the further concentration of the 10% contour of the three-dimensional reflectivity histogram into the diagonal zone of downward increasing reflectivity. The three-dimensional histogram of w (Fig 1h) shows diminishing updraft and downdraft velocities above 10 km. Between 5 and 10 km height the 10% contour of the three-dimensional histogram of Z continued to encompass a wide range of dBZ (from roughly 18 to 40) and this layer was also the the one in which the strongest updrafts and downdrafts were located. The level of maximum upper-level downdraft lowered in concert with the layer of maximum updraft. As a result, the upper-level downdraft and lower-level precipitation-

driven downdrafts were almost merged into a unimodal peak in the three-dimensional histogram. As the ice melted, it formed rain in a range of drop sizes, resulting in a broadening of the Z distribution below 5 km.

2237: By this time the convection was weakening throughout the volume of echo. The radar reflectivity pattern was losing its previous cellular character. Convective-scale up- and downdrafts, possibly remnants of previously stronger drafts, were still found throughout the echo volume but were considerably weaker than earlier. In the leading convective line the maximum drafts were ~5 m/s while in the trailing portion of the system they were ~1-2 m/s. The mean vertical velocity was ~ 0.5 m/s in the upper troposphere and —0.1 m/s in the lower troposphere. This mean vertical velocity profile is rather similar to that found in stratiform regions of mesoscale convective systems (Houze 1989). The three-dimensional histogram of vertical velocity (Fig. 1j) shows a distribution of vertical velocities much narrower than at previous times. Most of the volume of storm exhibits weak downdrafts below 5 km and weak updrafts above 5 km. The highly concentrated contours in the three-dimensional histogram of reflectivity (Fig. 1i) from 5 km upwards indicates that horizontal uniformity of reflectivity was tightening considerably compared to the 2155 volume. extending downward to the 5 km level. One can envision the ice particles growing, aggregating and melting during their decent. This increased uniformity in reflectivity structure indicates that the storm was in a stage where it was evolving toward a stratiform phase. However, the variability of vertical velocity as shown by the three-dimensional histogram of w (Fig. 1j) is not characteristic of a stratiform region. Evidently, the storm was in a transitional stage, in which the echo above the 0 deg C level was becoming more horizontal and stratiform-like but in which the decaying convection was still active enough for the vertical velocity field to be characterized as an ensemble of convective-scale up- and downdrafts.

4. CONCLUSIONS

Three-dimensional histograms of the ensemble properties of a radar volume provide key insights into Florida cumulonimbus of 15 August 1991. The 1% contour in the Z histograms shows enhancement of reflectivity at the 0 deg C level at early stages of storm development and prior to any radar bright band in vertical cross-sections. A characteristic progression in the reflectivity histograms is evident as the storm develops. An initial generally wide distribution of reflectivity values aloft evolves into a narrowly peaked distribution consistent with the more homogenous environment characteristic of the stratiform stage of the storm. The values of the peak in Z decrease markedly with height, giving the plotted distribution a diagonal peak in reflectivity-height coordinates. Surprisingly, this diagonalization of the distribution began when the convection was in its most vigorous stage.

The histograms of w show that strong upper-level downdrafts developed in direct association with the strongest updrafts. At the earliest time, the three-dimensional histogram of w shows that strong vertical velocities were present (Fig. 1b). Cells had not reached tropopause level. Strong downdrafts were beginning to appear in the middle troposphere, but upper-level downdrafts were not highly evident at this time. By 2139, the echo tops were nearing their maximum height, the bimodal character of the 1% contour on the downdraft side of the three-dimensional histogram of w was first appearing. By 2144 the bimodal structure was sharply defined. At both times, the upper-level downdraft peak was at the same height as the upper-level updraft peak. At 2144, this peak was at about 12 km. As the system began to weaken and the strong updrafts were peaking at about 8-10 km (2155-2237), the upper-level downdraft maximum also dropped to the 8-10 km level. The existence of strong mid- and upper-level downdrafts has been reported previously (Heymsfield and Schotz 1985, Smull and Houze 1987, Biggerstaff and Houze 1993, Knupp 1987, Kingsmill and Wakimoto 1991, and others). The temporally coincident appearance of the upper-level downdraft with the maximum of strong updraft occurrence is strong support for the hypothesis (Heymsfield and Schotz 1985) that the upper-level downdrafts are forced by the outflow from the strong updrafts. In other words, the upper level downdrafts are a consequence of the buoyancy perturbation pressure field created by the updrafts (Houze 1993, Chapter 7). Further support for the hypothesis is the systematic location of the upper-level downdrafts in relation to the updrafts. Inspection of vertical and horizontal cross sections indicates that the upper level downdrafts were ringing the updrafts.

In comparing the three-dimensional histogram time series to each other one is struck by the curious feature that the microphysical processes as represented by the Z data seem to be running on a faster time scale than the kinematic processes as represented by the w data. The microphysical evolution toward a homogenous stratified state appears to outpace the kinematic evolution into a stratiform region, characterized by weak downdraft below and weak updraft above the freezing level. Surprisingly, the storm begins to take on stratiform microphysical characteristics such as glaciation, enhancement of reflectivity at the freezing level and a diagonal trend (in dBZ-height space) of peak distributions, indicating that the majority of hydrometeors are increasing in size with descreasing height, all despite the intense churning up of the air by strong updrafts and downdrafts. Notwithstanding our perception from viewing cross-sections, where one's eyes are naturally drawn to the sharp peaks and strong magnitudes, even in very active convective storms much of the air has near zero vertical velocity (Fig. 1) and thus the microphysical processes of a more quiescent cloud dominate over the majority of the volume covered by the radar echo.

Acknowledgements

We appreciate the help of James Wilson, Matthias Steiner, Bradley Smull, John McCarthy, Brian Mapes, Andrew Detweiler, Jonathan Corbet, Christopher Burghardt, Scott Braun and Michael Biggerstaff. This research was supported by a NASA Space Grant Fellowship, an EOS Global Change Fellowship, NASA Grant NAG 5 1599, and the National Center for Atmospheric Research.

References

Biggerstaff, M. I. and R. A. Houze, Jr., 1991: *Mon. Wea. Rev.*,119, 3034-3065.

_____ and _____, 1993: *Mon. Wea. Rev., in press*

Foote, G.B. ed., 1991: *Scientific Overview and Operation Plan for the Convection and Precipitation/Electrification Experiment*, National Center for Atmospheric Research, Boulder.

Heymsfield, G.M. and S. Schotz, 1985: *Mon. Wea. Rev.*, 113, 1563-1589.

Houze, R. A., Jr., 1989: *Quart. J. Roy. Meteor. Soc.*, 115, 425-461.

Houze, R. A., Jr., 1993: *Cloud Dynamics*. Academic Press, San Diego, *in press*.

Kingsmill, D.E. and R. M. Wakimoto, 1991: *Mon. Wea. Rev*, 119, 262-297.

Knupp, K.R., 1987: *J. Atmos. Sci*, 44, 987-1008.

Smull, B. F. and R. A. Houze Jr., 1987: *J. Atmos. Sci.*, 44, 2128-2148.